

# An EOM-assisted wave-vector-resolving Brillouin light scattering setup

T. Neumann,\* T. Schneider, A. A. Serga, and B. Hillebrands  
*Fachbereich Physik and Forschungszentrum OPTIMAS*  
*Technische Universität Kaiserslautern, 67663 Kaiserslautern, Germany*  
(Dated: March 8, 2022)

Brillouin light scattering spectroscopy is a powerful technique which incorporates several extensions such as space-, time-, phase- and wave-vector resolution. Here, we report on the improvement of the wave-vector resolution by including an electro-optical modulator. This provides a reference to calibrate the position of the diaphragm hole which is used for wave-vector selection. The accuracy of this calibration is only limited by the accuracy of the wave-vector measurement itself. To demonstrate the validity of the approach the wave vectors of dipole-dominated spin waves excited by a microstrip antenna were measured.

PACS numbers: 78.35.+c, 75.30.Ds

## I. INTRODUCTION

Brillouin light scattering (BLS) spectroscopy is a versatile technique to investigate dynamic magnetic phenomena. Its power is significantly increased by numerous extensions which were added to the basic spectroscopic setup over time.

By introducing time-resolution, it was possible to investigate the evolution of a parametrically excited magnon gas in a ferrite film and observe the formation of a Bose-Einstein condensate of magnons at room temperature [1, 2]. The inclusion of space-resolution led to the discovery of important nonlinear wave phenomena such as soliton and bullet formation [3, 4], the observation of spin-wave tunneling [5] as well as spin-wave quantisation in nanoscaled structures [6].

Other discussed extensions comprise phase- [7] and wave-vector resolution [8]. The latter is particularly interesting since the frequency does usually not uniquely identify a wave eigenmode. Due to an often complex dispersion relation the additional knowledge of the wave vector is essential.

For the investigation of spin waves in ferrite films by BLS, wave-vector resolution was already introduced in the late 70's [9]. Subsequently, many studies (e.g. [10, 11, 12]) have copied the originally presented principle: to the BLS setup in forward scattering geometry a diaphragm is added in the beam path after the sample stage (see Fig. 1). Depending on the shape and position of the hole in the diaphragm, some components of the scattered laser beam which correspond to certain in-plane wave vectors are blocked while others can pass and are detected. The latest success of this technique was the time- and wave-vector resolved observation of a parametrically pumped magnon gas after pumping was switched off [13].

It is of crucial importance for an accurate measurement of the in-plane wave-vector to calibrate the position of the diaphragm hole. The zero position when the

elastically scattered beam passes through the diaphragm can be adjusted by sight, however this procedure is inevitably inaccurate. A second possibility is to calibrate the position based on the measured data: Stokes and anti-Stokes peaks in the BLS spectrum lead to two distinct signals with opposing wave vectors. Their symmetric position with respect to the center can in special cases be used for calibration. However, the intensities of Stokes and anti-Stokes peaks can differ greatly which makes this procedure difficult. Moreover, it is unnecessarily time-consuming since the weaker of the two signal peaks determines the accuracy of the calibration and, therefore, the required measurement time though in many cases it does not yield any additional physical information about the system under investigation.

The approach presented here uses an intrinsic calibration which is achieved by placing an electro-optical modulator (EOM) in the optical path behind the laser light source. The small amount of modulated, frequency-shifted light plays the role of a reference beam for the wave-vector resolution. Since it follows the same path as the unshifted laser light scattered inelastically from the sample but does (in first approximation) not undergo any inelastic scattering in the sample itself, it indicates the position where the in-plane wave vector vanishes for the measurement.

The proposed calibration procedure has two major advantages. First of all, it is applicable even when one of the two signals from Stokes and anti-Stokes scattering is not large enough to be observed. This is in particular the case for surface magnetostatic spin waves. Secondly, it potentially decreases the measurement time since the wave vector scanning does not have to be performed over the whole range of wave vectors but can (if a symmetry is already known) be restricted to one of the symmetric parts.

To test the validity of the presented method the in-plane wave vectors of propagating, dipole-dominated spin waves were resolved. The obtained results are in good quantitative agreement with theory.

It should be remarked that electro-optical modulators have already been used to realize phase resolution [7] and

---

\*Electronic address: neumann@physik.uni-kl.de

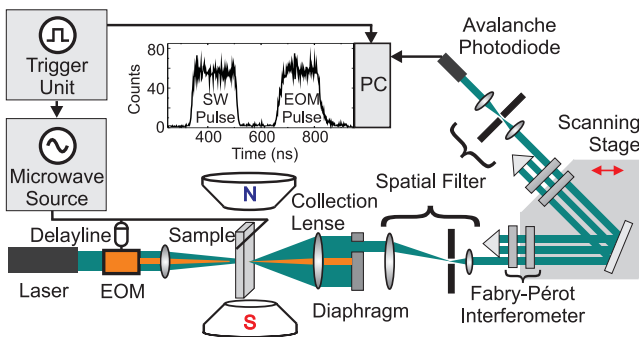


FIG. 1: (Color online) Sketch of the experimental setup.

enhance the frequency resolution [14]. This work adds to their increasing role for the improvement of the Brillouin light scattering setup.

## II. SETUP

The experimental setup is shown in Fig. 1. The sample under investigation consisted of a  $5 \mu\text{m}$  thick yttrium-iron-garnet (YIG) film which was tangentially magnetized by a magnetic field  $H$  (indicated by two pole pieces in Fig. 1). To a microstrip transducer on the surface of the YIG stripe a 200 ns long microwave pulse with 7.132 GHz carrier frequency was supplied with a  $1 \mu\text{s}$  repetition rate. The configuration was chosen in such a way that the microwave pulse excites a packet of backward volume magnetostatic spin waves (BVMSW) which propagates in the film in the direction of the bias magnetic field [15, 16]. Thus, the in-plane wave vector of the excited spin waves has a well defined, unique non-zero component. The measurements discussed below focus on determining the wave number of this wave.

To detect the spin-wave packet light from a single mode, frequency-stabilized 532 nm laser was focused on the sample close to the antenna. The transmitted light was sent to a (3+3)-pass tandem Fabry-Pérot interferometer where the frequency of the light inelastically scattered from the spin waves was resolved. A good description of the underlying BLS setup is found in [17].

The existing BLS setup already includes time- and space resolution in the following way: In order to probe different points of the sample, the sample is mounted on a stage which can be moved by a stepper motor. Time resolution is achieved by measuring the time between the launch of the microwave signal pulse which excites the spin-wave packet and the detection of the scattered photons by the detector. In the current setup the time resolution is limited to 1.8 ns due to the finesse of the Fabry-Pérot etalons. A detailed account is given in [18].

Wave-vector resolution was added to the existing setup by placing a diaphragm with a central hole of 0.5 mm diameter in the focal plane behind the collection lens. The diaphragm was mounted on a stage which was horizon-

tally movable by a PC-controlled stepper motor. The stage was moved in steps of size 0.08 mm. Since the investigated spin waves possessed only one non-vanishing in-plane component of the wave-vector the chosen one-dimensional approach is sufficient for demonstration. To measure both in-plane wave-vector components an additional stage for the vertical displacement of the diaphragm will be added. The measurement principle remains, however, unchanged.

To calibrate the diaphragm position, an EOM was placed in the beam path in front of the sample (see Fig. 1). It was driven by a 200 ns long pulse from the same microwave source that generated the spin-wave pulse. However, the EOM-pulse was delayed compared to the spin-wave pulse in order to make EOM and spin-wave signal clearly distinguishable in the time-resolved measurements.

Since the same microwave frequency is applied to the EOM and the microstrip transducer which excites the spin waves, the resulting signal peaks in the BLS spectrum coincide. This has two practical advantages. First of all, the frequency interval which is effectively scanned by the interferometer can be small. This reduces the overall measurement time which is particularly important for wave-vector resolved measurements. Secondly, the EOM-signal can be used as a frequency reference [14].

## III. EXPERIMENTAL RESULTS

Figure 2 shows the intensity of the detected BLS signal relative to the elapsed time and the displacement of the diaphragm from its initial (arbitrary) position. Three signals are clearly distinguishable:

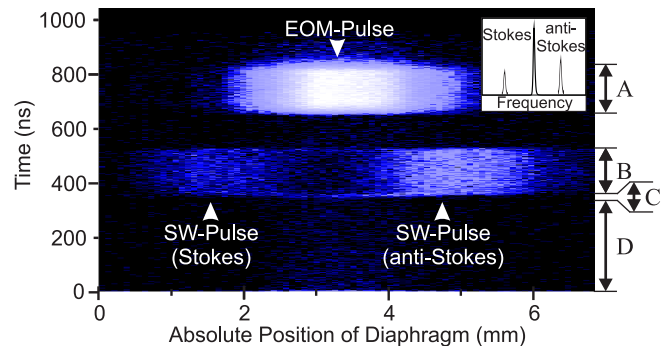


FIG. 2: (Color online) Time-resolved intensity of the scattered light with respect to the displacement of the diaphragm for a bias magnetic field  $H = 4\pi 1.870 \text{ Am}^{-1}$  and a spin-wave carrier frequency  $f = 7.132 \text{ GHz}$ . Indicated are the signals from EOM reference pulse in the time interval A as well as from the spin-wave (SW) packet corresponding to the Stokes- and anti-Stokes-peak in the BLS spectrum (sketched in inset) observed in the time interval B. The thermal signal received during the transition period C together with the signal measured during the transition period D is shown in the different panels of Fig. 5.

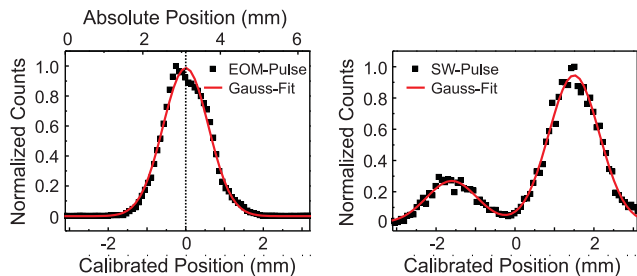


FIG. 3: (Color online) Dependence of the BLS signal obtained for the EOM pulse and the SW pulse on the diaphragm displacement. The lines are the results of Gauss fits.

In the time interval marked in Fig. 2 as *A* the signal from the EOM-pulse is seen. The time interval *B* contains two signals which both stem from the propagating spin-wave packet. They correspond to the Stokes and anti-Stokes peaks in the BLS spectrum. This was checked by restricting the BLS measurement once to the Stokes and once to the anti-Stokes peak (see inset in Fig. 2). In particular, the position of the signals corresponding to Stokes and anti-Stokes BLS peaks exchanged their positions when the laser beam was focused on the other side of the exciting microstrip antenna where the spin-wave packet travels in the opposite direction and the spin-wave wave vector, therefore, changes sign.

To increase the signal to noise ratio the received counts were integrated over the time intervals *A* and *B*, respectively. The resulting intensity distribution, which depends only on the diaphragm displacement, is shown in Fig. 3. It is relatively wide because of the comparatively large pin hole in the diaphragm. However, this trade-off was accepted to decrease the measurement time. By fitting the experimental data with a single Gaussian distribution for the EOM-signal and two independent Gaussian distributions with the same variance for the spin-wave signal, the accuracy of the measurement was enhanced. As can be seen from Fig. 3, the fits agree well with the experimental data. The center of the Gaussian profile which fits the EOM-signal was used to calibrate the diaphragm displacement and obtain the  $k = 0$  – position for the diaphragm. Relative to this position the deflection  $x$  of the beam which was inelastically scattered on the spin-wave packet was determined.

Measurements were performed for different magnetic fields with the same spin-wave carrier frequency 7.132 GHz. The results are presented in Fig. 4. Figure 4(a) shows extracts corresponding to the interval *B* in Fig. 2 which contains the information on the spin-wave wave vector. In accordance with theory an almost linear field dependence is seen [16].

In order to unambiguously resolve the signals corresponding to the Stokes and anti-Stokes peaks in the BLS spectrum, separate measurements were conducted by limiting the spectral scanning to one of the two spectral positions (Panel (b)).

From the data, the spin-wave wave number  $k_{\text{SW}}$  is ob-

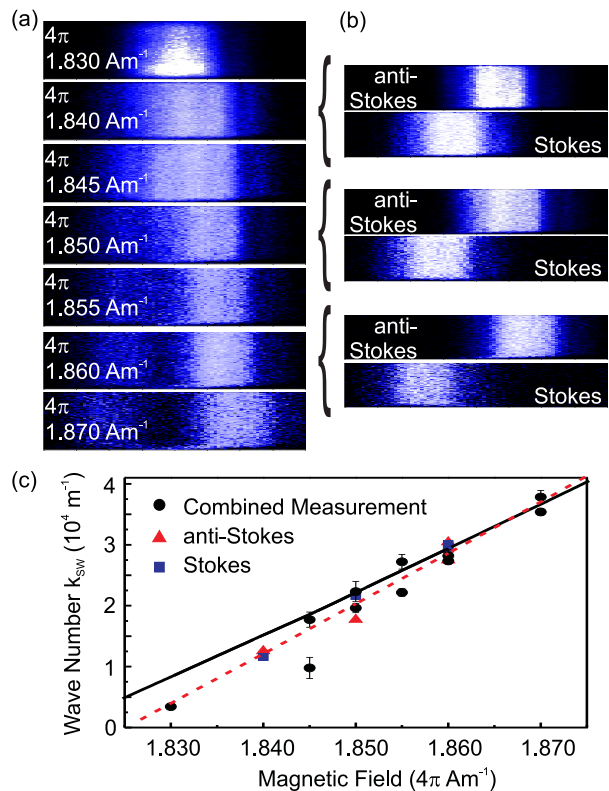


FIG. 4: (Color online) Dependence of the observed signal on the bias magnetic field indicated in each panel. (a) Spatial signal distribution when Stokes and anti-Stokes are measured together (compare to Fig. 2). (b) Separately measured Stokes and anti-Stokes signals. (c) Experimentally obtained wave numbers in comparison with theoretical calculations without fit parameters (solid line) and with adjusted magnetic field and film thickness (dashed line).

tained using the Bragg-condition

$$k_{\text{SW}} = 2 \cdot k_{\text{Laser}} \sin(\vartheta/2) = 2 \cdot k_{\text{Laser}} \sin\left(\frac{\arctan(x/f)}{2}\right)$$

where  $k_{\text{Laser}} = 1.181 \times 10^7 \text{ m}^{-1}$  is the wave number of the incoming laser light and  $\vartheta$  is the angle between the elastically and inelastically scattered light which is determined by the focal length  $f = 500 \text{ mm}$  of the collection length and the measured deflection  $x$  of the spin-wave signal. The experimentally found spin-wave numbers  $k_{\text{SW}}$  are combined in Fig. 4(c) with theoretical calculations based on the Damon-Eshbach formula for the lowest order BVMSW mode [16]. The solid line has been calculated based on the measured field value, a film thickness of  $5 \mu\text{m}$  and a saturation magnetisation  $4\pi\mu_0 M_s = 0.175 \text{ T}$ . In comparison, the dashed line is the result of a fit, where the film thickness and the magnetic field were taken as fit parameters. The optimal value found for the thickness was  $4.2 \mu\text{m}$ , the magnetic field was adjusted by a shift  $\Delta H = -4\pi \cdot 0.007 \text{ Am}^{-1}$  relative to the experimentally measured field  $H$ . Both deviations are within reasonable range. The film thickness is not

known with sufficient accuracy and is in general assumed as a fit parameter. The experimentally measured magnetic field does not take into account any contributions from the crystalline anisotropy.

Overall, the theoretical curves agree well with experiment. The measurements indicate that the film thickness at the point of the laser focus was less than the nominal  $5 \mu\text{m}$ .

#### IV. DISCUSSION

The presented results confirm the validity of the EOM-assisted wave-vector resolution measurement procedure. The EOM allows an easy, intrinsic calibration with the same resolution as the actual measurement. The calibration does not rely on any symmetry in the observed peaks and can be performed even when the scanning is restricted to one side of the BLS spectrum. The widely adjustable intensity of the EOM beam guarantees a minimal expenditure of time to obtain a large enough signal for the analysis.

In principle, the EOM beam can be used to calibrate the diaphragm prior to the experiment. Instead, in the presented work the EOM reference was applied parallel to the actual measurement. This is a natural solution whenever the pulse regime is required because of other experimental restrictions. The reference EOM beam is applied during the dead time of the cycle so that the overall duration of the experiment is not increased and measurement as well as calibration are completed in a single run.

The experiments confirmed the applicability of the diaphragm-based approach to wave-vector resolution for the measurement of small wave numbers. The method is not the only way to go in this regime. It is also possible to measure the spin-wave wavelength by using phase resolution [7]. However, this method relies on the scanning of the sample which does, in terms of measurement time not yield any advantages. Moreover, it is only applicable in the case of a single spin wave propagating under homogeneous external conditions - fast temporal or spatial variations of the wave number cannot be resolved. The same draw-backs apply to other interference-based methods using, for instance, inductive probes.

For the diaphragm-approach these limitations do not apply: Since the method relies on the measurement at a single point on the sample, inhomogeneities in the sample do not play any role. As has been seen above, it is even possible to distinguish waves with the same wave-number modulus but travelling in opposite directions.

In combination with the time-resolution it is possible to resolve the wave-number evolution. This is shown in Fig. 5 where the measured wave vector distribution for different time intervals is presented when the front of the spin-wave packet passed the laser spot.

The integrated signal from the interval marked as  $D$  in Fig. 2 is presented in Panel (I). The observed

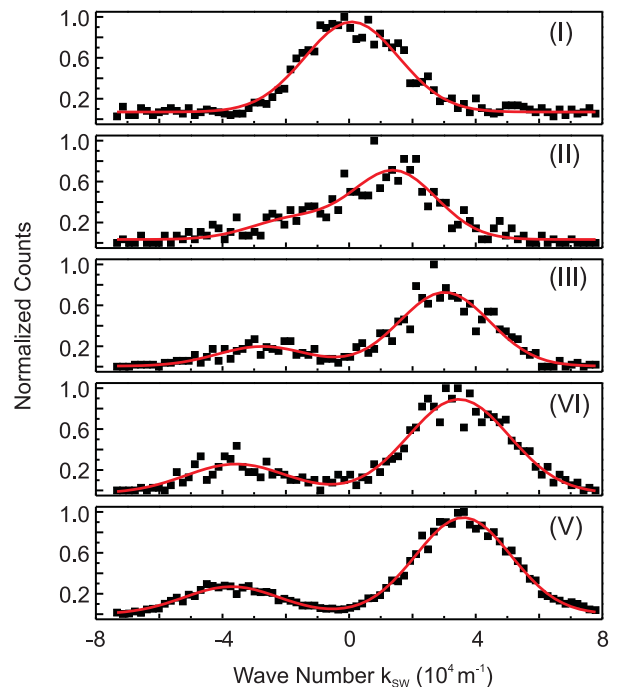


FIG. 5: (Color online) Time-resolved wave-number measurements (■) together with Gaussian fits (solid line). (I) Thermal signal from interval  $D$  in Fig. 2. (II)-(IV) Consecutive measurements when the pulse front passes the laser spot (see  $C$  in Fig. 2). (V) Spin-wave signal from  $B$  in Fig. 2

peak with an experimentally measured wave number of  $k_{\text{FMR}} = (900 \pm 700) \text{ m}^{-1}$  corresponds to the thermally excited uniform mode in the sample. Panels (II)-(IV) contain the measured wave-vector distributions for three consecutive, 8.7 ns long time intervals at the moment when the front of the pulse passed the laser spot and was detected. These time slices are taken from the interval denoted by  $C$  in Fig. 2. Panel (V) finally shows the wave-vector distribution for interval  $B$  when the measured signal intensity and the wave-vector distribution have reached a stable regime. By comparing the panels, the different wave-number contributions at the front of the pulse due to the dispersion of the spin-wave packet can be distinguished. It is in qualitative agreement with the phase profile of a linear spin-wave packet, which exhibits characteristic distortions at the front and end of the pulse [7].

#### V. CONCLUSION

In conclusion, we have improved the existing wave-vector resolution used in Brillouin light scattering experiments by including an electro-optical modulator as a reference to calibrate the position of the diaphragm hole. The EOM beam makes it possible to determine the position where the in-plane wave vector vanishes with an accuracy comparable to the accuracy of the actual wave-

vector measurement itself. For experiments conducted in the pulse regime, the proposed method does not increase the measurement time but even cuts it in half under optimum conditions. The applicability of the EOM-based calibration was tested by measuring the wave vectors of a propagating packet of dipole-dominated spin-waves for different bias magnetic fields with time resolution. Comparison with the established theory showed a good agreement.

## VI. ACKNOWLEDGEMENTS

This work has been financially supported by the Matcor Graduate School of Excellence, the Graduiertenkolleg 792, and the DFG within the SFB/TRR 49.

- 
- [1] S. O. Demokritov, V. E. Demidov, O. Dzyapko, G. A. Melkov, A. A. Serga, B. Hillebrands, and A. N. Slavin, *Nature* **443**, 430 (2006).
  - [2] V. E. Demidov, O. Dzyapko, S. O. Demokritov, G. A. Melkov, and A. N. Slavin, *Phys. Rev. Lett.* **100**, 047205 (2008).
  - [3] M. Bauer, O. Büttner, S. O. Demokritov, B. Hillebrands, V. Grimalsky, Yu. Rapoport, and A. N. Slavin, *Phys. Rev. Lett.* **81**, 3769 (1998).
  - [4] A. A. Serga, M. P. Kostylev, and B. Hillebrands, *Phys. Rev. Lett.* **101**, 137204 (2008).
  - [5] S. O. Demokritov, A. A. Serga, A. André, V. E. Demidov, M. P. Kostylev, and B. Hillebrands, *Phys. Rev. Lett.* **93**, 047201 (2004).
  - [6] H. Schultheiss, S. Schäfer, P. Candeloro, B. Leven, B. Hillebrands, and A. N. Slavin, *Phys. Rev. Lett.* **100**, 047204 (2008).
  - [7] A. A. Serga, T. Schneider, B. Hillebrands, S. O. Demokritov, and M. P. Kostylev, *Appl. Phys. Lett.* **89**, 063506 (2006).
  - [8] Hua Xia, P. Kabos, H. Y. Zhang, P. A. Kolodin, and C. E. Patton, *Phys. Rev. Lett.* **81**, 449 (1998)
  - [9] V. N. Venitskiĭ, V. V. Eremenko, and É. V. Matyushkin, *Sov. Phys. JETP* **50**, 934 (1979).
  - [10] W. Wettling, W. D. Wilber, P. Kabos, and C. E. Patton, *Phys. Rev. Lett.* **51**, 1680 (1983).
  - [11] P. Kabos, G. Wiese, and C. E. Patton, *Phys. Rev. Lett.* **72**, 2093 (1994).
  - [12] P. Kabos, M. Mendik, G. Wiese, and C. E. Patton, *Phys. Rev. B* **55**, 11457 (1997).
  - [13] V. E. Demidov, O. Dzyapko, M. Buchmeier, T. Stockhoff, G. Schmitz, G. A. Melkov, and S. O. Demokritov, *Phys. Rev. Lett.* **101**, 257201 (2008).
  - [14] S. Caponi, M. Dionigi, D. Fioretto, M. Mattarelli, L. Palmieri, and G. Socino, *Rev. Sci. Instrum.* **72**, 198 (2001).
  - [15] R. W. Damon and Eshbach, J. R., *J. Phys. Chem. Solids* **19**, 308 (1961).
  - [16] M. J. Hurben and C. E. Patton, *J. Magn. Magn. Mater.* **139**, 263 (1995).
  - [17] B. Hillebrands, *Rev. Sci. Instrum.* **70**, 1589 (1999).
  - [18] O. Büttner, M. Bauer, S. O. Demokritov, B. Hillebrands, Yu. S. Kivshar, V. Grimalsky, Yu. Rapoport, and A. N. Slavin, *Phys. Rev. B* **61** 11576 (2000).